Polskie Towarzystwo Materiałów Kompozytowych
Polish Society of Composite Materials

25: 2 (2025) 58–66

COMPOSITES THEORY AND PRACTICE

ISSN (online): 2299-128X

Pradeep Kumar Karsh[1], Satnam Singh[2*], Anamol Gautam[3], Durgesh Kumar Mishra[4], Dhowmya Bhatt[5], Navin Kumar[6]

[1] *Department of Mechanical Engineering, Parul Institute of Engineering and Technology, Parul University, Vadodara, India*
[2] *Department of Mechanical Engineering, National Institute of Technology Kurukshetra, Haryana, India*
[3] *Department of Applied Science, Chandigarh Engineering College, Chandigarh Group of Colleges Jhanjeri, Mohali Punjab, India*
[4] *Department of Aeronautical Engineering, Hindustan Institute of Technology and Science, Chennai, India*
[5] *Department of Computer Science and Engineering, SRM Institute of Science and Technology, Delhi NCR Campus, Ghaziabad*
[6] *Department of Mechanical Engineering, Rashtrakavi Ramdhari Singh Dinkar College of Engineering, Begusarai, India*
[*] *Corresponding author e-mail:* endless550@gmail.com

Received (Otrzymano) 19.10.2024

INVESTIGATION OF SPECIFIC WEAR RATE AND WEAR MECHANISM IN STIR CAST AL5052 COMPOSITES WITH TIB_2 AND ZRO_2 REINFORCEMENTS

https://doi.org/10.62753/ctp.2025.07.2.2

In this work, Al5052 alloy was reinforced with varying weight percentages of titanium diboride (TiB_2) and zirconium dioxide (ZrO_2) to fabricate three hybrid composite samples (S1, S2, and S3) via the stir casting process. Dry sliding wear tests were conducted using a pin-on-disc apparatus under varying loads (10, 20, and 30 N) and sliding speeds (300, 500, and 700 rpm), with a constant sliding distance of 1500 m. The results showed that the specific wear rate (SWR) grew with increasing load, reaching a maximum of 3.45×10^{-4} mm³/N·m for sample S1 at 30 N. Among the samples, S3 exhibited the best wear resistance, with the lowest SWR of 1.35×10^{-4} mm³/N·m under identical conditions. SEM analysis revealed different wear mechanisms such as mild ploughing in S1, crack formation in S2, and plastic deformation in S3. These findings demonstrate that the hybrid reinforcement of TiB_2 and ZrO_2 significantly improves the wear resistance of Al5052, making it suitable for applications in automotive and aerospace sectors requiring enhanced surface durability.

Keywords: specific wear rate, wear mechanism, stir casting, aluminum alloys, metal matrix composite

INTRODUCTION

The wear behavior of composite materials is a critical factor influencing their performance and longevity in engineering applications [1]. Wear, defined as the gradual removal of material from a surface due to mechanical interactions such as sliding, abrasion, or impact, is particularly important in composites where both the matrix and reinforcement play crucial roles. The wear resistance of a composite depends on several factors, including the type of matrix (metallic, polymeric, or ceramic), the nature and volume fraction of the reinforcement (such as fibers, particulates, or whiskers), and the interfacial bonding between the matrix and reinforcement [2]. Composites can experience different wear mechanisms such as abrasive wear, where hard particles scratch or cut the surface; adhesive wear, involving material transfer due to localized bonding; erosive wear from high-speed particle impacts; and delamination wear, which is common in layered or laminated composites [3]. Reinforcements like silicon carbide (SiC), alumina (Al_2O_3), and graphite significantly

enhance the wear resistance of composites by increasing the hardness and reducing friction. Furthermore, uniform distribution of reinforcement and strong interfacial bonding are essential for minimizing material loss under operational stresses [4]. Owing to their excellent wear resistance, composites have found wide-ranging applications across several industries. In the aerospace sector, composites are used in components such as rotor blades, landing gear parts, and wear-resistant seals, offering high strength-to-weight ratios in addition to enhanced durability. In the automotive industry, wear-resistant composites are commonly employed in brake pads, clutch plates, pistons, and engine liners, where they provide improved performance under frictional and thermal stresses. The defense sector utilizes advanced composites for lightweight yet durable armor panels and structural components that endure harsh conditions [5]. In industrial applications, composites serve in machinery parts like bearings, gears, and wear plates where high reliability and low maintenance are crucial. The medical field also benefits from wear-resistant polymer matrix composites in joint replacements and prosthetic devices. These widespread applications underscore the importance of tailoring composite materials to meet specific wear demands across diverse engineering domains. The evolution of composite materials has been driven by the need to enhance material properties beyond those offered by conventional materials. Initially developed for aerospace and defense applications in the mid-20th century, composites have since evolved through the integration of advanced manufacturing techniques such as powder metallurgy, additive manufacturing, and surface modification technologies [6]. The continuous innovation in reinforcements – ranging from natural fibers to nanoscale materials like graphene and carbon nanotubes – has led to composites with superior wear resistance, mechanical strength, and thermal stability. Their importance lies not only in their ability to reduce weight and improve fuel efficiency but also in extending the service life of components under demanding conditions. As industries continue to seek materials that combine lightweight characteristics with high durability, wear-resistant composites will play an increasingly vital role in modern engineering solutions.

Aluminum alloys are among the most widely used engineering materials because of their excellent strength-to-weight ratio, corrosion resistance, good formability, and recyclability [7]. These alloys are classified broadly into two categories: wrought alloys (processed by rolling, extrusion, or forging) and casting alloys (formed by pouring molten metal into molds). The alloys are further grouped into heat-treatable and non-heat-treatable types based on how their mechanical properties are enhanced. The evolution of aluminum alloys began in the early 20th century, with the development of the Duralumin series (Al-Cu) for aviation applications. Over time, advancements in alloying techniques led to the creation of high-strength series such as 2xxx (Al-Cu) and 7xxx (Al-Zn-Mg-Cu), which became essential for aerospace and defense. In parallel, alloys like 5xxx (Al-Mg) and 6xxx (Al-Mg-Si) were developed for structural and automotive applications due to their good corrosion resistance and weldability [8]. Modern developments include aluminum-lithium alloys for weight reduction in aerospace and aluminum matrix composites (AMCs) reinforced with ceramics or particles to enhance wear, thermal, and mechanical properties. The applications of aluminum alloys are vast and span across several industries. In the aerospace sector, high-strength alloys like 2024, 7075, and aluminum-lithium composites are used in fuselage skins, wing structures, and landing gear as a consequence of their excellent strength and fatigue resistance [9]. The automotive industry uses 5xxx and 6xxx series alloys in car bodies, chassis, and engine components to reduce vehicle weight as well as improve fuel efficiency [10]. In construction, aluminum alloys are employed for roofing, window frames, and structural glazing because of their corrosion resistance and ease of fabrication. Marine applications rely on corrosion-resistant alloys like 5083 and 5456 for hulls and superstructures [11]. Additionally, aluminum alloys are used in electrical transmission lines, packaging, consumer electronics, and sports equipment. The ongoing research into alloy

design, processing, and surface treatment continues to expand the functionality and sustainability of aluminum alloys, making them integral to modern manufacturing and engineering solutions.

MATERIALS AND METHODS

The commercially available Al5052 alloy was selected as the matrix material for this investigation due to its excellent corrosion resistance, moderate strength, and good workability. The chemical composition of Al5052, determined via spectroscopic analysis, is presented in Table 1. The alloy primarily consists of aluminum as the base element, with notable additions of magnesium (2.233 wt%), iron (0.230 wt%), and silicon (0.122 wt%), along with trace amounts of chromium, manganese, copper, and zinc. To reinforce the matrix, titanium diboride (TiB_2) and zirconium dioxide (ZrO_2) nanoparticles were employed. TiB_2 nanoparticles, with an average particle size (APS) of up to 80 nm and a purity of 99.9%, were sourced from Intelligent Materials Pvt. Ltd., Punjab. ZrO_2 nanoparticles, with an APS ranging between 30–50 nm and a purity of 99.9%, were procured from Nano Research Lab, Jamshedpur. These reinforcements were selected for their exceptional hardness, thermal stability, and proven effectiveness in enhancing the mechanical and tribological properties of aluminum matrix composites.

TABLE 1. **Composition of matrix material**

Element	Si	Fe	Cu	Mn	Mg	Cr	Zn	Al
Content	0.12%	0.23%	0.02%	0.07%	2.23%	0.15%	0.07%	Remainder

The fabrication process began with melting of the commercially available Al5052 alloy in a graphite crucible using an electric resistance furnace [12]. The alloy was heated to a temperature of approximately 750°C, which is slightly above its melting point (~615°C), to ensure complete melting and fluidity for uniform mixing. Before adding the reinforcement particles, the molten aluminum was subjected to degassing using an inert gas, typically argon or nitrogen, bubbled through the melt for 10–15 minutes. This step effectively removed dissolved hydrogen gas and other impurities, reducing porosity and improving the quality of the final composite [13]. The TiB_2 and ZrO_2 nanoparticles were preheated separately to around 300°C to eliminate moisture and enhance wettability with the molten matrix. The reinforcements were then gradually introduced into the semi-solid slurry at about 650°C under vigorous mechanical stirring at 400–600 rpm to promote uniform dispersion and minimize particle agglomeration. After thorough mixing for 10–15 minutes, the temperature was carefully controlled and maintained to avoid premature solidification. The molten composite slurry was then poured into preheated steel molds maintained at 200–250°C to reduce thermal shock and ensure controlled solidification [14]. The cooling rate was optimized to achieve a fine-grained microstructure, enhancing the mechanical strength and wear resistance. The entire process was conducted under an inert atmosphere or in a controlled environment to prevent oxidation and contamination of the melt.

To evaluate the dry sliding wear behavior of the Al5052-based nanocomposites, a DUCOM pin-on-disc wear testing machine was employed, following the ASTM G99 standard for test conditions and sample preparation [15]. The composite samples were fabricated in the form of square pins, each measuring 25 mm in height and 10 mm in width. These pins were tested against an EN-31 steel disc with a diameter of 200 mm and a hardness of 62 HRC, which acted as the counterface material. Prior to testing, all the samples underwent a sequential polishing process utilizing emery papers of grit sizes 220, 400, 600, 1000, 1500,

and 2000 to ensure uniform and smooth contact surfaces, minimizing surface irregularities that could influence wear behavior [16]. The wear tests were conducted under dry conditions with a constant track diameter of 60 mm, and each run was performed for a duration of 15 minutes. During the test, the wear rate was determined by measuring the mass loss of the pin samples before and after testing, and the wear mechanism was evaluated by morphological examination. Subsequent to the wear tests, SEM analysis was carried out to study the worn surface morphology of the samples. The samples analyzed included: S1 (99% Al5052 + 1% TiB_2), S2 (99% Al5052 + 1% ZrO_2), and S3 (98% Al5052 + 1% TiB_2 + 1% ZrO_2). Before and after each wear test, the rotating EN-31 steel disc and the composite pin samples were carefully cleaned with acetone and tissue paper to eliminate any surface contaminants, ensuring accurate and consistent measurements. A total of 27 wear experiments were conducted, with each of the three composite samples (S1, S2, and S3) undergoing nine distinct test conditions. To ensure reliability and reduce experimental variability, each test was repeated three times, and the average wear rate was computed and recorded for analysis. The consistent cleaning procedure and repetition of tests under controlled conditions enhanced the accuracy and reproducibility of the experimental data. The specific test parameters, including applied load, sliding speed, and sliding distance, are detailed in Table 2.

TABLE 2. **Test parameters along with their respective levels**

Parameters	Level 1	Level 2	Level 3
Applied load (N)	10	20	30
Sliding speed (m/s)	0.94	1.57	2.20
Sample designation	S1	S2	S3

RESULTS AND DISCUSSION

Wear results

The wear behavior of the fabricated aluminum matrix composites (AMCs) was assessed by means of a pin-on-disc apparatus by calculating the mass loss and determining the specific wear rate (SWR), using the standard formulation given by Eqs. 1 and 2:

$$\text{SWR}=\frac{\text{Mass loss}}{\text{Density} \times \text{Sliding distance} \times \text{Load}}\ \text{mm}^3/\text{N-m} \quad (1)$$

$$\text{Sliding distance (m)} = \text{Sliding speed} \times \text{time} \quad (2)$$

Figures 1 through 3 depict the variation in the wear rate with different applied loads (10 N, 20 N, and 30 N) and sliding speeds (0.94 m/s, 1.57 m/s, and 2.2 m/s). The following sections elaborate the effects of load and speed on the specific wear rate.

Effect of load on wear rate of Al5052 composites

The test results reveal a consistent trend where the SWR increases with increasing applied load up to 30 N, indicating a corresponding reduction in wear resistance. At the sliding speed of 0.94 m/s and 1.57 m/s, the hybrid composite S3 (98% Al5052 + 1% TiB_2 + 1% ZrO_2) exhibited the lowest SWR at 10 N, as shown in Figures 1 and 2. This suggests superior wear resistance in the hybrid formulation. However, when the load was increased to 30 N, the SWR for S3 rose sharply to 1.482×10^{-4} mm³/N·m at 0.94 m/s (Fig. 2), likely resulting from severe particle-matrix debonding and microstructural deformation.

Interestingly, at the higher sliding speed of 2.2 m/s under a 10 N load (Fig. 3), S3 demonstrated an SWR of 1.316×10^{-4} mm³/N·m, which was higher than S2 (1% ZrO_2), which recorded 1.007×10^{-4} mm³/N·m. This unexpected result may be attributed to voids, porosity, or nanoparticle agglomeration in the hybrid sample, reducing its tribological efficiency under specific operating conditions.

Effect of sliding speed on wear rate of Al5052 composites

Figure 4 illustrates that the SWR initially increased with sliding speed at the fixed load of 30 N, but decreased as the speed was increased from 1.57 m/s to 2.2 m/s. This trend is in line with findings by Arunbharathi et al. [17], who reported enhanced wear resistance in hybrid metal matrix composites at higher speeds and sliding distances. At lower speeds, adhesive wear mechanisms dominate as a consequence of the prolonged contact time, resulting in greater material removal. As the speed increases, abrasive wear mechanisms take over, which often leads to smoother surfaces and reduced wear rates.

The lowest SWR was recorded at 0.94 m/s, highlighting the effectiveness of lower speeds in controlling wear. Comparatively, previous studies demonstrated similar outcomes. For instance, the reinforcement of Al6061 with 3% graphene nanoplatelets (GNPs) and 3% CeO_2 yielded a minimum SWR of 0.303 mm³/N·m [15]. Mahmut et al. tested Al/GNP composites and observed a minimum SWR of 1.2×10^{-4} mm³/N·m at 10 N and 1.8×10^{-4} mm³/N·m at 40 N [18]. Similarly, Sharma et al. reported a minimum SWR of 2×10^{-4} mm³/N·m for Al6101/graphite composites reinforced with 4% graphite, affirming the advantage of hybrid and nanoscale reinforcement in enhancing tribological performance [19].

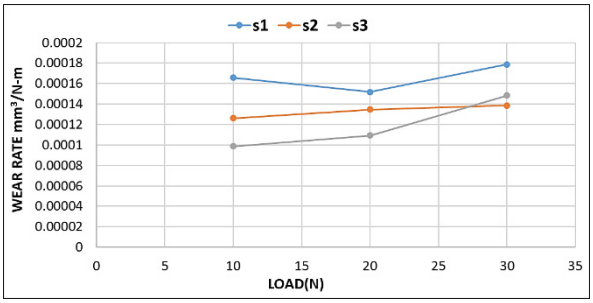

Fig. 1. Change in SWR with load at 0.94 m/s

The graph above illustrates the variation in the wear rate (mm³/N·m) with respect to the applied load (N) for the three different composite samples – S1 (Al5052 + 1% TiB_2), S2 (Al5052 + 1% ZrO_2), and S3 (Al5052 + 1% TiB_2 + 1% ZrO_2) – evaluated under dry sliding conditions by means of the pin-on-disc wear test. S1 (Al5052 + TiB_2) consistently exhibits the highest wear rate across all the loads (10 N, 20 N, and 30 N). This indicates relatively lower wear resistance compared to the other two composites. The wear rate slightly decreases at 20 N but grows again at 30 N, showing a nonlinear response. S2 (Al5052 + ZrO_2) shows a more stable wear rate trend, with only a modest rise as the load increases. This suggests that ZrO_2 contributes effectively to wear resistance, likely due to its high hardness and thermal stability. S3 (Al5052 + TiB_2 + ZrO_2) initially has the lowest wear rate at 10 N, demonstrating superior wear resistance owing to the synergistic effect of both reinforcements. Nevertheless, as the load increases to 30 N, the wear rate of S3 rises and becomes nearly equal to that of S2, likely because of increased surface damage and possible agglomeration of nanoparticles at higher loads.

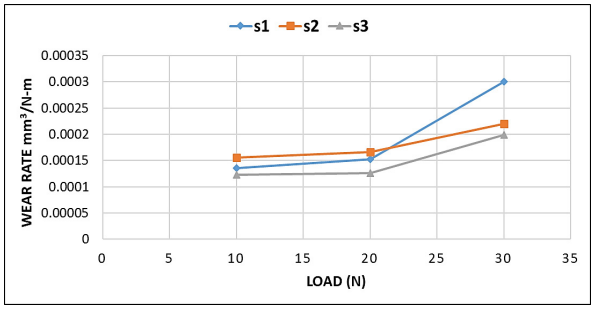

Fig. 2. Change in SWR with load at 1.57 m/s

As observed in Figure 2, all the samples exhibit growth in the wear rate with increasing load, which is consistent with typical wear behavior under elevated normal forces. Among the three, the S1 sample shows the highest wear rate, especially at 30 N, where it peaks at approximately 0.00032 mm³/N·m, suggesting that TiB_2 reinforcement alone is less effective at high loads. In contrast, the S3 hybrid composite consistently demonstrates the lowest wear rate up to 20 N, indicating enhanced wear resistance resulting from the synergistic effect of the dual nanoparticle reinforcement. Nonetheless, its wear rate also rises significantly at 30 N, though it remains lower than that of S1. The S2 composite maintains moderate wear performance across all the load levels, suggesting that ZrO_2 provides better load-bearing ca-

pacity and stability than TiB_2 when used individually. Overall, the hybrid composite (S3) offers superior wear resistance at lower to moderate loads, making it a promising candidate for applications demanding both strength and durability.

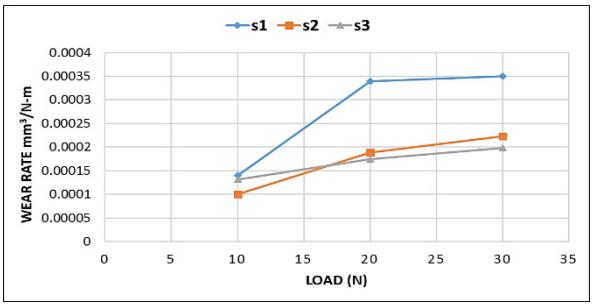

Fig. 3. Change in SWR with load at 2.2 m/s

It is evident in Figure 3 that the wear rate of all the samples grows progressively with the rise in applied load, which is a typical trend due to the intensified contact pressure and heat generation at higher loads. Among the samples, S1 consistently exhibits the highest SWR across all the loading conditions, peaking close to 0.00038 mm³/N·m at 30 N, indicating that TiB_2 alone is less effective in resisting wear under high-stress conditions. On the other hand, both S2 and S3 show significantly lower wear rates, with S2 performing slightly better than S3 at the lower and medium loads. This suggests that ZrO_2 contributes effectively to wear resistance, possibly owing to its high hardness and toughness. S3, the hybrid composite, also demonstrates improved performance over S1, particularly at higher loads, indicating the beneficial effect of combining TiB_2 and ZrO_2. Overall, the incorporation of ZrO_2 – either individually or in hybrid form – substantially improves the wear resistance of the Al5052 matrix, making it more suitable for load-bearing applications.

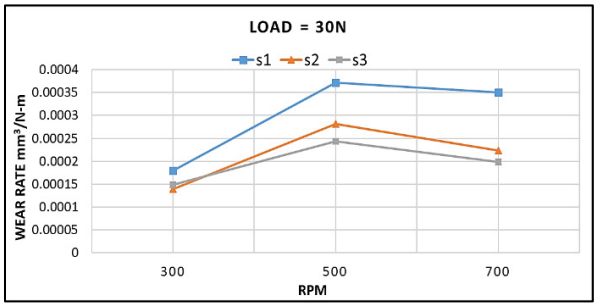

Fig. 4. Change in SWR with speed at 30 N load with change in sliding speed (m/s)

The graph in Figure 4 represents the specific wear rate (SWR) of the Al5052-based composites under a constant applied load of 30 N at varying rotational speeds: 300, 500, and 700 rpm. The data shows that the wear rate initially increases with speed from 300 rpm to 500 rpm, followed by a decrease at 700 rpm for all the samples. This pattern suggests that at medium speed (500 rpm), adhesive wear and thermal effects become more pronounced, resulting in greater material loss. Among all the samples, S1 consistently exhibits the highest wear rate across all the speeds, reaching a maximum of approximately 0.00037 mm³/N·m at 500 rpm. In contrast, S3 demonstrates the lowest wear rate, particularly at 700 rpm, indicating superior wear resistance, likely resulting from the synergistic effect of TiB_2 and ZrO_2 reinforcements that enhance hardness and reduce plastic deformation. S2 shows intermediate wear behavior, better than S1 but slightly less effective than S3. These findings imply that hybrid reinforcement significantly improves the wear resistance of Al5052 composites, especially at higher sliding speeds, making them more suitable for applications involving severe tribological conditions.

Surface morphology

EDX analysis

The EDX spectra of the TiB_2 and ZrO_2 powders are shown in Figs. 5 and 6 respectively.

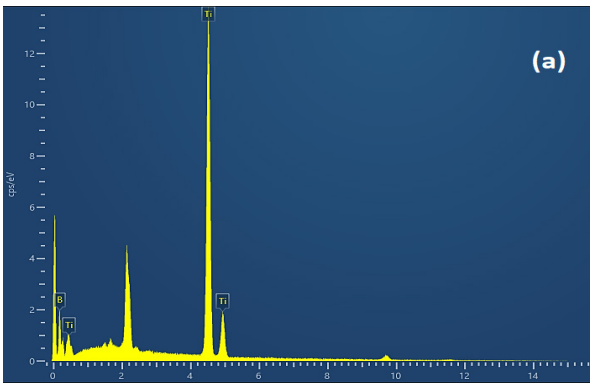

Fig. 5. EDX spectrum of TiB2

In Figure 5, the prominent peaks observed in the spectrum correspond to titanium (Ti) and boron (B), confirming the presence of TiB_2 nanoparticles in the sample. The dominant titanium peaks

around 4.5 keV and smaller peaks for boron near 0.2 keV suggest a higher content of titanium compared to boron, consistent with the stoichiometric nature of TiB_2. The clear identification of these elements validates the successful incorporation of TiB_2 nanoparticles into the aluminum matrix, as intended in the composite fabrication process.

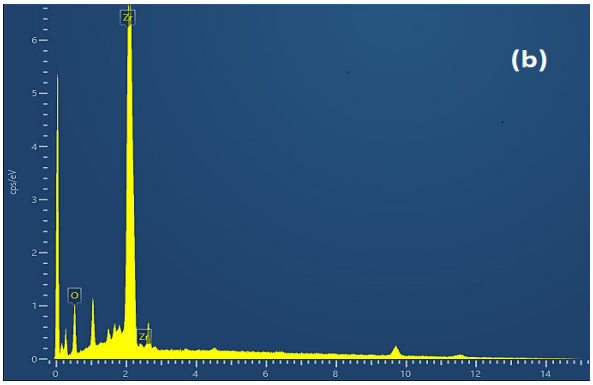

Fig. 6. EDX spectrum of ZrO2

Two distinct peaks are prominently visible in Figure 6: the major peak at around 2 keV and 15.8 keV, which corresponds to zirconium (Zr), and a smaller peak near 0.5 keV, which is attributed to oxygen (O). The high intensity of the Zr peaks suggests that zirconium is the dominant element, while the oxygen peak confirms the oxide form of the compound – ZrO_2. This EDX spectrum confirms the successful incorporation of the zirconium dioxide nanoparticles in the material. The detection of both zirconium and oxygen in the expected ratios validates the integrity and purity of the ZrO_2 reinforcement, which was introduced into the aluminum matrix to enhance the mechanical and thermal properties in the composite system.

SEM analysis of wear surfaces

The SEM micrograph (Figure 7) of the worn surface of the S1 sample (Al5052 reinforced with 1% TiB_2) at 200× magnification reveals distinct features characteristic of adhesive and abrasive wear mechanisms. The surface shows visible ploughing marks, which are long, parallel grooves formed by hard asperities or wear debris scratching along the sliding direction. These grooves suggest the dominance of abrasive wear where material is displaced rather than removed. Additionally, mild patches are observed across the worn surface, indicating localized plastic deformation and adhesion during sliding. The presence of such patches implies intermittent sticking between the sample and the counter disc, followed by tearing, which is typical of adhesive wear. These surface features suggest that under the applied tribological conditions, the S1 sample experienced moderate wear, with both abrasive ploughing and mild adhesion contributing to material loss. The absence of significant cracks or severe delamination also confirms that the wear is mild to moderate rather than catastrophic.

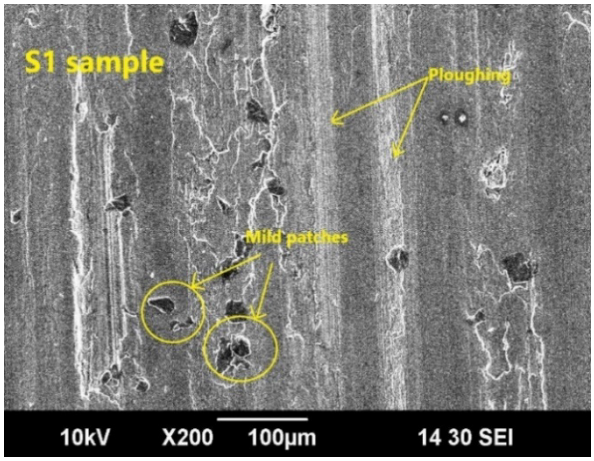

Fig. 7. SEM micrograph of S1 sample

The SEM micrograph (Figure 8) of the S2 sample (Al5052 reinforced with 1% ZrO_2) at 200× magnification displays a worn surface marked by the presence of micro-cracks and localized surface damage. The most notable feature is the clear formation of cracks within the circled region, suggesting that the material has undergone considerable stress during the wear test. These cracks are indicative of a brittle wear mechanism, likely resulting from the hard and brittle nature of the ZrO_2 particles, which can initiate microcracking under repeated mechanical loading. The overall surface appears rough and fragmented, further reinforcing the idea that the reinforcement led to localized stress concentration points, promoting crack propagation. Compared to S1, the wear

mechanism in S2 is more severe due to crack formation, implying lower toughness and a transition towards more brittle wear behavior.

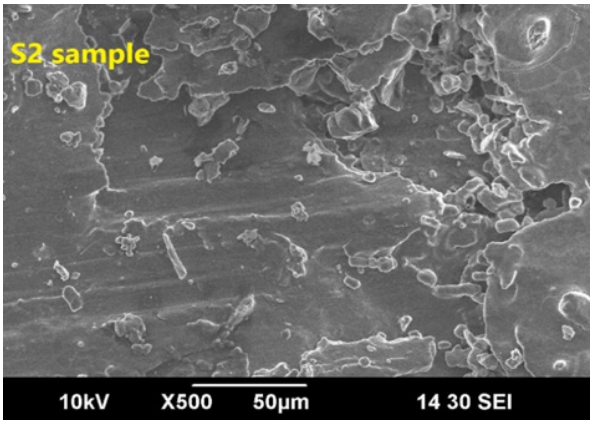

Fig. 8. SEM micrograph of S1 sample

The SEM micrograph (Figure 9) of the S3 sample at 500× magnification reveals a surface characterized by prominent plastic deformation features. Unlike the S2 sample, the wear surface appears smoother, with noticeable flow lines indicative of material displacement rather than brittle fracture. The marked plastic deformation suggests that the material has absorbed and accommodated the applied stress through ductile mechanisms, which contributes to enhanced wear resistance. The absence of severe cracks or fragmented debris indicates better bonding and load distribution within the composite, likely because of the combined reinforcement of TiB2 and ZrO2 nanoparticles in S3. This synergy results in a more resilient surface capable of sustaining sliding contact without significant material loss from brittle failure. The plastic deformation also implies that the composite can dissipate frictional heat and mechanical energy more effectively, reducing the severity of wear. Overall, the S3 sample demonstrates improved wear performance through ductile wear mechanisms and reduced crack propagation, which aligns with its lower specific wear rate in the tests. This microstructural behavior highlights the advantage of hybrid reinforcement in optimizing the balance between hardness and toughness in the Al5052-based composites.

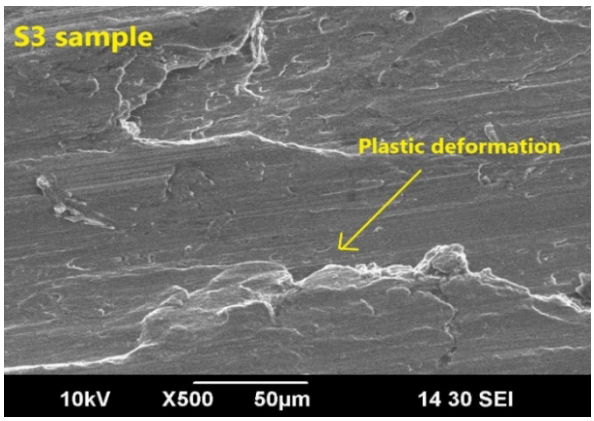

Fig. 9. SEM micrograph of S1 sample

CONCLUSIONS

The tribological behavior of Al5052-based composites reinforced with varying combinations of TiB_2 and ZrO_2 was thoroughly investigated under different loads and sliding speeds. The wear rate trends and surface morphology were analyzed to understand the dominant wear mechanisms. Based on the experimental observations, the following conclusions were drawn:

1. The wear rate grows with the applied load and sliding speed, but the extent varies across the samples resulting from the different reinforcement compositions.
2. The S3 sample exhibited the lowest wear rate, indicating superior wear resistance due to the synergistic effect of the TiB_2 and ZrO_2 hybrid reinforcements.
3. The S1 sample showed mild ploughing and patch formation, pointing to abrasive wear and weaker surface integrity under load.
4. The S2 sample exhibited crack formation, suggesting a more brittle wear mechanism likely owing to the presence of single reinforcement (TiB_2).
5. S3 sample demonstrated plastic deformation, indicating a ductile wear mechanism with better energy absorption and reduced surface damage.
6. The SEM analysis confirms that hybrid reinforcement (TiB_2 + ZrO_2) enhances the tribological performance by reducing crack propagation and improving surface integrity under sliding conditions.

REFERENCES

[1] H. Nautiyal, S. Kumari, O. P. Khatri, R. Tyagi, 'Copper matrix composites reinforced by rGO-MoS2 hybrid: Strengthening effect to enhancement of tribological properties', *Composites Part B: Engineering*, vol. 173, no. May, p. 106931, 2019, DOI: 10.1016/j.compositesb.2019.106931.

[2] D. Kumar, S. Singh, S. Angra, 'Effect of reinforcements on mechanical and tribological behavior of magnesium-based composites : a review', vol. 50, no. 3, pp. 439–458, 2022, DOI: 10.18149/MPM.5032022.

[3] S. Singh, S. Angra, 'Experimental evaluation of hygrothermal degradation of stainless steel fibre metal laminate', *Engineering Science and Technology, an International Journal*, vol. 21, no. 1, pp. 170–179, 2018, DOI: 10.1016/j.jestch.2018.01.002.

[4] E. Omrani, P.L. Menezes, P.K. Rohatgi, 'State of the art on tribological behavior of polymer matrix composites reinforced with natural fibers in the green materials world', *Engineering Science and Technology, an International Journal*, vol. 19, no. 2, pp. 717–736, 2016, DOI: 10.1016/j.jestch.2015.10.007.

[5] D. Kumar, S. Angra, S. Singh, 'Mechanical Properties and Wear Behaviour of Stir Cast Aluminum Metal Matrix Composite: A Review', *International Journal of Engineering, Transactions A: Basics*, vol. 35, no. 4, pp. 794–801, 2022, DOI: 10.5829/IJE.2022.35.04A.19.

[6] S. Wakeel, A.A. Khan, 'REVIEW ARTICLE A REVIEW ON THE MECHANICAL PROPERTIES OF ALUMINIUM BASED METAL MATRIX * Saif Wakeel and Ateeb Ahmad Khan', vol. 6, pp. 1096–1100, 2017.

[7] D. Kumar, 'Qualitative and quantitative interdependence of physical and mechanical properties of stir-casted hybrid aluminum composites', vol. 51, no. 6, pp. 14–23, 2023, DOI: 10.18149/MPM.5162023.

[8] M. Jafarian, M. Saboktakin, 'A Comprehensive Study of Diffusion Bonding of Mg AZ31 to Al 5754, Al 6061 and Al 7039 Alloys', *Transactions of the Indian Institute of Metals*, vol. 71, no. 12, pp. 3011–3020, 2018, DOI: 10.1007/s12666-018-1402-0.

[9] M. Alloying, 'Microstructure and Compressive Behavior of Al–Y 2 O 3 Nanocomposites Prepared by Microwave-Assisted Mechanical Alloying', 2019.

[10] T. Article, 'The Corrosion Behavior of Graphene-Reinforced Al Matrix Composites in 3 . 5 wt .% NaCl Solution', vol. 32, no. June, pp. 5176–5185, 2023, DOI: 10.1007/s11665-022-07452-6.

[11] S. Ozden, R. Ekici, F. Nair, 'Investigation of impact behaviour of aluminium based SiC particle reinforced metal-matrix composites', *Composites Part A: Applied Science and Manufacturing*, vol. 38, no. 2, pp. 484–494, 2007, DOI: 10.1016/j.compositesa.2006.02.026.

[12] J. Petrovi, S. Mladenovi, I. Markovi, S. Dimitrijevi, 'CHARACTERIZATION OF HYBRID ALUMINUM COMPOSITES REINFORCED WITH Al 2 O 3 PARTICLES AND WALNUT-SHELL', vol. 56, no. 2, pp. 115–122, 2022, DOI: 10.17222/mit.2022.365.

[13] D. Kumar, S. Angra, S. Singh, 'Synthesis and characterization of DOE-based stir-cast hybrid aluminum composite reinforced with graphene nanoplatelets and cerium oxide', *Aircraft Engineering and Aerospace Technology*, vol. 95, no. 10, pp. 1604–1613, 2023, DOI: 10.1108/AEAT-04-2023-0104.

[14] A. Subburaj, A. Marcel, M. Antony, J. Decruz, 'Mechanical Characterization and Micro-structural Analysis on AA2024 Hybrid Composites Reinforced with WC and Graphene Nanoparticles', *Transactions of the Indian Institute of Metals*, vol. 75, no. 7, pp. 1721–1730, 2022, DOI: 10.1007/s12666-021-02488-z.

[15] D. Kumar, S. Singh, S. Angra, 'Dry sliding wear and microstructural behavior of stir-cast Al6061-based composite reinforced with cerium oxide and graphene nanoplatelets', *Wear*, vol. 516–517, no. September 2022, p. 204615, 2023, DOI: 10.1016/j.wear.2022.204615.

[16] D. Kumar, S. Angra, S. Singh, 'High-temperature dry sliding wear behavior of hybrid aluminum composite reinforced with ceria and graphene nanoparticles', *Engineering Failure Analysis*, vol. 151, no. May, p. 107426, 2023, DOI: 10.1016/j.engfailanal.2023.107426.

[17] R. Arunbharathi, R. Rathish, R.S. Vignesh, P.S. Seelan, R. V. Prasanth, 'Mechanical and Tribological Characteristics of Particulates Embedded Aluminium Based Composites – A Review', vol. XIV, no. 3, pp. 12–16, 2021.

[18] M. C. Senel, 'Dry Sliding Wear and Friction Behavior of Graphene / ZrO 2 Binary Nanoparticles Reinforced Aluminum Hybrid Composites', pp. 9253–9269, 2022, DOI: 10.1007/s13369-022-06661-4.

[19] A. Sharma, S. Kumar, G. Singh, O. P. Pandey, 'Effect of particle size on wear behavior of al-garnet composites', *Particulate Science and Technology*, vol. 33, no. 3, pp. 234–239, 2015, DOI: 10.1080/02726351.2014.954686.